Chin. Sci. Bull. (2014) 59(26):3232–3238
DOI 10.1007/s11434-014-0413-4

csb.scichina.com
www.springer.com/scp

Article

Condensed Matter Physics

Hydrogen induced room-temperature ferromagnetism in Co-doped ZnO: first-principles and Monte Carlo study

Jian-Min Zhang · Zhigao Chen · Kehua Zhong · Guigui Xu · Zhigao Huang

Received: 11 December 2013 / Accepted: 11 February 2014 / Published online: 24 May 2014

Abstract The structural stability, vibrational and magnetic properties of hydrogen doped ZnO:Co have been studied by first-principles calculations based on density functional theory. Bond-center (BC) sites were identified to be most stable sites for hydrogen, the corresponding vibrational frequencies including anharmonic contributions were calculated. Its magnetic properties were investigated as well. The calculated results reveal that hydrogen could induce the change of electronic transfer, leading to a decrease of magnetic moment. However, the magnetic coupling between Co atoms is greatly strengthen. The results simulated by Monte Carlo method indicate that hydrogen can induce the Curie temperature to increase from 200 to 300 K.

Keywords Diluted magnetic semiconductors · First principles calculation · Monte Carlo simulation

1 Introduction

ZnO-based diluted magnetic semiconductors (DMS) have attracted considerable attention for their potential applications in spintronics and microelectronics in the few years [1]. Since Ueda's work on room temperature ferromagnetism (RTFM) for $Zn_{1-x}Co_xO$ was published [2], room-temperature ferromagnetism (FM) has commonly been obtained in ZnO doped with Mn [3, 4], Co [5–8], Ni [9, 10], V [11–13], Cr [14–16] and Fe [17, 18]. However, the origin of ferromagnetism in Co-doped ZnO material is still controversial [19]. Some groups suggested that the observed FM was an intrinsic property [20, 21], while Risbud and Lawes et al. [22, 23] found no ferromagnetism in Co-doped polycrystalline ZnO. Moreover, the issue of hydrogen in ZnO was extensively investigated [24–28]. It is noteworthy that hydrogen is commonly present in the crystal growth environment and inevitably incorporates into ZnO crystal. First-principles calculations carried out by Van de Walle [29] revealed that interstitial hydrogen in ZnO acts as a shallow donor. Subsequently, theoretical and experimental efforts confirmed further the existence of the shallow donor hydrogen state in zinc oxide [30, 31]. Furthermore, it was suggested that H can mediate a strong short-range spin–spin interaction between magnetic ions in $Zn_{1-x}Co_xO$, leading a high temperature ferromagnetism [24]. Experimental studies indicated that H played an important role in the enhancement of ferromagnetic spin-spin interactions that went much beyond a carrier-mediated effect [25, 26]. Recently, the electrical and magnetic properties of low-energy H^+-implanted ZnO single crystals with hydrogen concentrations up to $\sim$3 at% have been investigated [31]. The hydrogen-induced ferromagnetism in H-ZnO samples is demonstrated by the magnetization and magnetotransport measurements [32]. Moreover, the magnetism of hydrogen-treated ZnO:Co was supported experimentally by magnetic measurements as well as theoretically by first-principles calculation [33]. They found that the two most favorable configurations are those where the H atoms reside at the Co-O bond center (BC) sites, namely $BC_{\parallel}$ and $BC_{\perp}$. It was suggested that one possible mechanism for the ferromagnetism is hydrogen-facilitated interaction, and H plays an important role in inducing

J.-M. Zhang · Z. Chen · K. Zhong · G. Xu · Z. Huang
College of Physics and Energy, Fujian Normal University, Fuzhou 350108, China

J.-M. Zhang · Z. Chen · K. Zhong · G. Xu · Z. Huang (✉)
Fujian Provincial Key Laboratory of Quantum Manipulation and New Energy Materials, Fuzhou 350108, China
e-mail: zghuang@fjnu.edu.cn

ferromagnetism. Therefore, it is crucial to get a deep understanding of the microscopic and electronic properties for hydrogen in Co-doped ZnO.

In this paper, we carry out first-principles calculation to study the structural stability of $Zn_{1-x}Co_xO$ and achieve the local vibrational modes of hydrogen-related complexes. It is significant to identify the microscopic configuration and helpful to experimental studies by infrared and Raman spectroscopy. Moreover, the magnetic properties of $Zn_{1-x}Co_xO$ induced by hydrogen are investigated. Finally, Monte Carlo method was employed to calculate Curie temperatures of hydrogen-doped ZnO-based DMSs.

2 Model and calculation

2.1 First-principles calculations

The total energy and vibrational frequencies calculations have been performed using density functional theory (DFT) [34] with the projected augmented wave (PAW) [35] potentials as implemented in the Vienna *ab initio* simulation package (VASP) [36, 37]. The cutoff energy for the plane wave expansion of electron wavefunction was set at 520 eV. A gamma-centered 3×3×2 k mesh was adopted to sample the irreducible Brillouin zone for 3×3×2 ZnO supercell. All atoms in each doped supercell were fully relaxed using the conjugate-gradient algorithm until the maximum force on a single atom was less than 0.02 eV/Å.

Schematic representation for possible hydrogen sites in wurtzite ZnO is shown in Fig. 1. As in ZnO, interstitial H acts as a shallow donor (H^+) [38]. AB_N (antibonding Nitrogen) and BC (bond center) configurations can be distinguished for the wurtzite structures [39]. There exist two types of configurations for AB_N and BC: one type is long to the c axis (labeled as $BC_{\parallel}$ and $AB_{N,\parallel}$), the other type is "perpendicular" to the c axis (labeled as $BC_{\perp}$ and $AB_{N,\perp}$). Considering the possibility of H near to dopant, $OA_{\parallel}$, $OA_{\perp}$ and $AB'_{N,\parallel}$ sites are proposed as well [40].

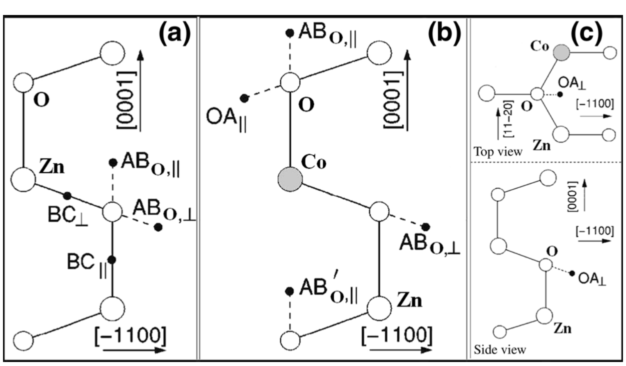

Fig. 1 Schematic representation of possible hydrogen sites in the (11–20) plane of wurtzite ZnO

The oscillation potential of H, $V(x)$, can be described as follows:

$$V(x) = \frac{k}{2}x^2 + \alpha x^3 + \beta x^4, \tag{1}$$

where the coefficient of the quadratic term gives the harmonic frequency $\omega^0 = \sqrt{k/\mu}$, where reduced mass μ is defined as: $\frac{1}{\mu} = \frac{1}{m_H} + \frac{1}{m_O}$, here m_H and m_O are the masses of the hydrogen and oxygen atoms, respectively.

Higher order coefficients α and β describe anharmonic contributions. Moreover, the Schrödinger equation of one-dimensional single-particle is described by

$$\left[-\frac{\hbar^2}{2\mu}\nabla^2 + V(x)\right]\psi(x) = E\psi(x). \tag{2}$$

Based on the perturbation theory [40, 41], an approximate analytical solution for the equation above can be obtained as follows:

$$\omega = \omega^0 + \Delta\omega = \sqrt{\frac{k}{\mu} - 3\frac{\hbar}{\mu}\left[\frac{5}{2}\left(\frac{\alpha}{k}\right)^2 - \frac{\beta}{k}\right]}, \tag{3}$$

where ω is the total frequency, ω^0 is the harmonic frequency, and $\Delta\omega$ is the anharmonic contribution.

2.2 Monte Carlo method

The Curie temperatures for magnetic study will be calculated using the Monte Carlo simulation with the magnetic atoms distributed randomly. We construct $L\times L\times L$ (L=16, 20 and 32) wurtzite ZnO with periodic boundary conditions. The ratios of ferromagnetic Co and non-magnetic Zn atoms are assumed to be x and $(1-x)$, respectively. Meanwhile, it is assumed that the Co atoms are distributed randomly on the Zn lattice sites of wurzite ZnO.

The Heisenberg Hamiltonian of the system will be described as

$$E = -\sum_{ij} J_{ij}\vec{S}_i\cdot\vec{S}_j - K\sum_i(\vec{S}_i\cdot\vec{u}_i) - H\sum_i S_i^z, \tag{4}$$

where J_{ij} is the exchange coupling constant. In this study, we label one Co atom as '0' with its neighbor Co atom labeled from 1 to 7, as can be seen in Fig. 2. $J_{0j} = J_{ij}$ (j = 1, 2, 3, 4, 5, 6, 7) represents the exchange coupling constant between the ith and jth Co atoms. The first, second and third terms in Eq. (4) are the exchange interactional energy, anisotropic energy, and Zeeman energy, respectively [42, 43]. The thermodynamic magnetization per atom and the susceptibility can be calculated by

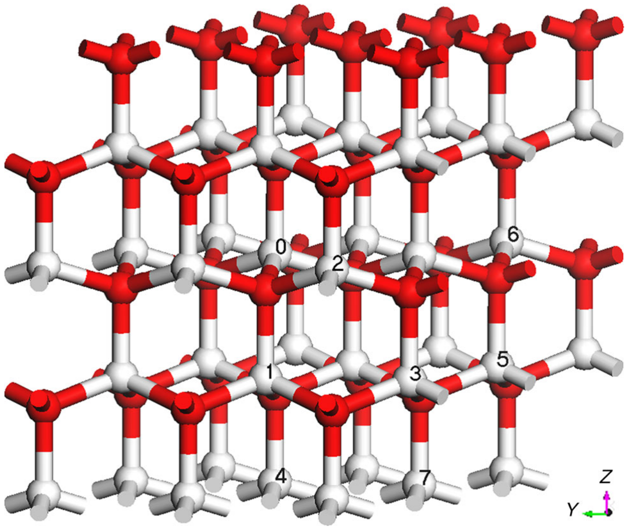

Fig. 2 (Color online) The 3×3×2 supercell of wurtzite ZnO containing 36 Zn atoms (*light*) and 36 O atoms (*dark*), and 7 Zn atoms in different sites are labeled

$$M(T) = < \left[\left(\sum_i S_i^x \right)^2 + \left(\sum_i S_i^y \right)^2 + \left(\sum_i S_i^z \right)^2 \right]^{1/2} > /N, \tag{5}$$

$$\chi(T) = N(<M^2> - <M>^2)/T, \tag{6}$$

where N is the number of the magnetic Co atoms. In order to define the Curie temperature, an accumulation of magnetization of the fourth order U_L is described as follows

$$U_L(T) = 1 - <M^4> /3<M^2>^2. \tag{7}$$

The maximum slope in U_L from the T dependence can be used for evaluation of the transition temperature. The χ–T and U_L–T curves are used to define the Curie temperature [44, 45]. In the simulation, we set $K = 0$, $H = 0.00086$ eV.

3 Results and discussion

We first examine the energetics of H incorporation in Co-doped ZnO. One Zn atom substituted by Co in 3×3×2 ZnO was investigated to indentify the stable configuration. The calculated total energy differences ΔE, bond lengths of O–H and vibrational frequencies for different configurations of O–H in Co doped ZnO are listed in Table 1. From the table, it is found that H favors the bond-center (BC) sites, and $BC_\perp$ is the most stable site while $BC_\parallel$ is the metastable state with ΔE = 0.02 eV. This result is consistent with the previous prediction [24, 29, 32]. The relaxed bond length of O–H for all the candidate configurations are approximate 1 Å.

Table 1 The calculated total energy differences ΔE, bond lengths of O–H and vibrational frequencies for different configurations of O–H, and the lowest energy is set as zero reference value

Sites	ΔE (eV)	$d_{O\text{–}H}$ (Å)	Mag (μ_B)	ω^0 (cm^{-1})	$\Delta\omega$ (cm^{-1})	ω (cm^{-1})
$BC_\perp$	0.00	0.997	3.0000	3774	−271	3503
$BC_\parallel$	0.20	1.006	3.0001	3720	−258	3462
$OA_\perp$	0.34	0.990	3.0167			
$OA_\parallel$	0.35	0.991	3.0234			
$AB'_{O,\parallel}$	0.41	0.992	3.0227			
$AB_{O,\perp}$	0.42	0.990	3.0002			
$AB_{O,\parallel}$	0.45	0.990	3.0015			

Considering the anharmonic contribution, we get the vibrational frequencies with 3503 and 3462 cm^{-1} for H at $BC_\perp$ and $BC_\parallel$ site, respectively. Clearly, the calculated results of structural stability for H-doped $Zn_{1-x}Co_xO$ are significant to experimentally probe, being crucial to our subsequent study of magnetic property.

We first investigate the Co-doped ZnO without hydrogen doping, getting a magnetic moment of 3.07 μ_B. Then, from Table 1 it is found that the magnetic moments of all configurations slightly reduced when hydrogen is embedded, especially for $BC_\perp$ site. It is obvious that hydrogen will induce a change of magnetism in Co-doped ZnO. Thus, a deep study of electronic transfer and magnetic coupling will be carried out.

A 3×3×2 supercell of ZnO with one Zn atom substituted by Co atom is shown in Fig. 3, corresponding to a doped concentration of 2.78 %. A hydrogen atom is doped

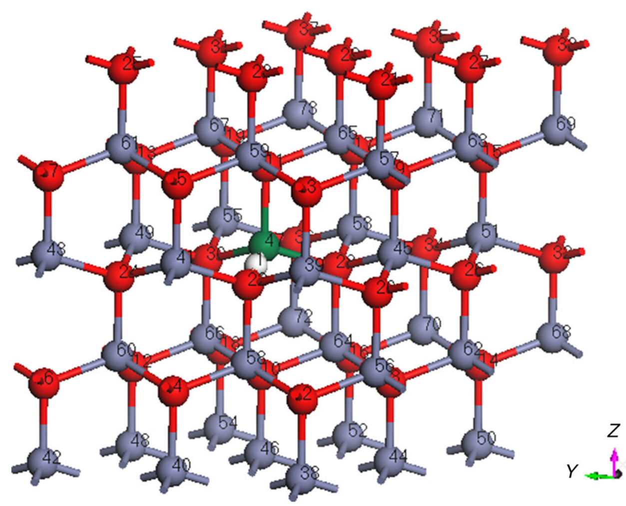

Fig. 3 (Color online) 3×3×2 supercell of ZnO with hydrogen in the interstitial $BC_\perp$ site. All the atoms are labeled from 1 to 73, containing 36 Zn atoms (*light*), 36 O atoms (*dark*), 1 Co atom (numbered 47) and 1 H atom (numbered 1)

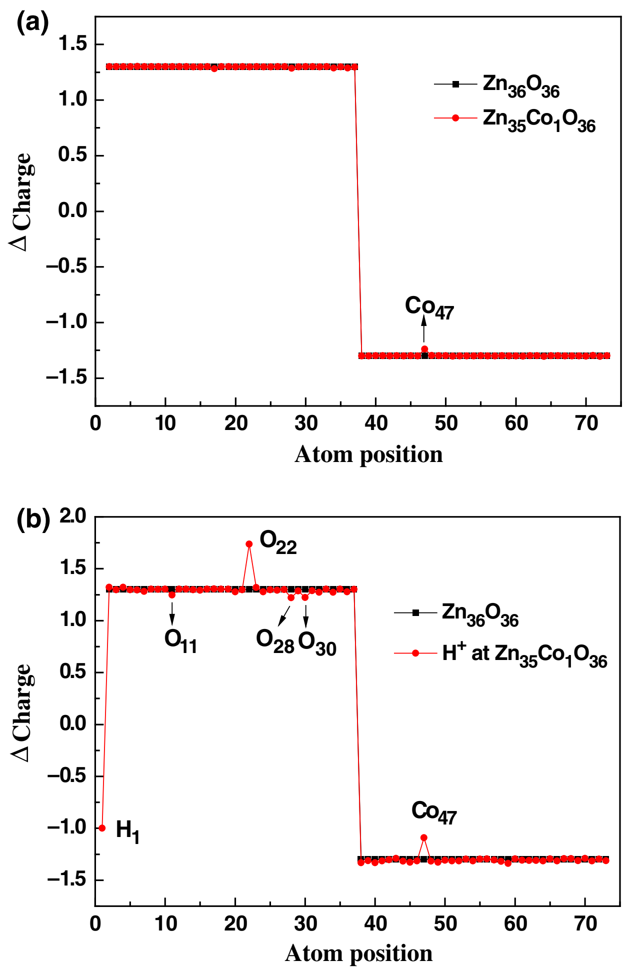

Fig. 4 (Color online) The electronic transfer structures for **a** $Zn_{1-x}Co_xO$ ($x = 2.78$ %) and pure ZnO; **b** $Zn_{1-x}Co_xO$ ($x = 2.78$ %) with H^+ in $BC_\perp$ site and pure ZnO

in the most stable interstitial site $BC_\perp$. All the 73 atoms are labeled from 1 to 73. Figure 4(a) and (b) show the electron transfer structures of single Co doped ZnO without and with hydrogen doped, respectively. From Fig. 4(a), it is found that for pure ZnO each Zn atom loses about 1.30 electrons while each O atom gets about 1.30 electrons. For the $Zn_{1-x}Co_xO$ ($x = 2.78$ %), Co atom has a obvious electron transfer and loses 1.24 electrons, which results in a slight electron transfer of its neighbor O atoms. From Fig. 4(b), it is observed that as hydrogen is doped, the electronic structure has a significant change. Due to the electrical activity, hydrogen readily incorporates with the 22nd O atom. The hydrogen loses 1.0 electrons, inducing a increase of electronic transfer for O_{22} atom to 1.74. Moreover, compared to Fig. 4(a), it is found that the number of the lost electrons for the other three O atoms (numbered 11, 28 and 30) bonding with Co is decreased. Co atom loses only 1.09 electrons, which gives rise to the weaken of the coupling between Co and O_{22} atoms.

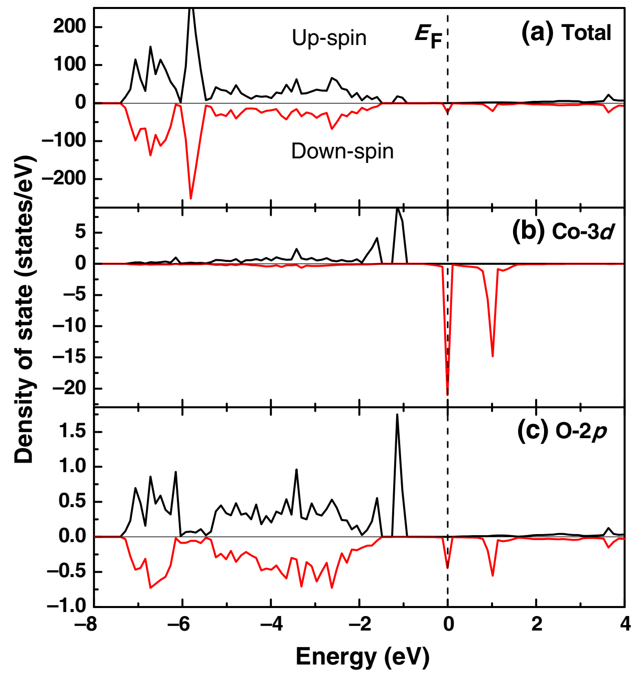

Fig. 5 (Color online) **a** Total density of states (DOS) and **b** Co-3*d* and **c** O-2*p* projected density of states (PDOS) of $Zn_{1-x}Co_xO$ ($x = 2.78$ %) (3×3×2 supercell) without hydrogen doped. The Fermi level (*dashed line*) is set as the zero energy. Positive (negative) values correspond to the majority (minority) spin

The total density of states (DOS) and projected density of states (PDOS) of $Zn_{1-x}Co_xO$ ($x = 2.78$ %) (3×3×2 supercell) without hydrogen doping are shown in Fig. 5, respectively. From the figure, a half-metallic behavior can be found with the majority spin being semiconducting and minority spin being metallic. The spins of conduction electrons at the Fermi level are almost 100 % polarized. Comparing the total DOS with the PDOS of the Co atom, it is found that most of the spin polarization states originate from Co-3*d* electrons. In addition, a hybridization between the Co-3*d* and O-2*p* bands is observed in the vicinity of the Fermi level. Therefore, the strong coupling between O-2*p* and Co-3*d* is mainly responsible for the ferromagnetic ground state in Co-doped ZnO before hydrogen is doped. Figure 6 shows the total density (DOS) and projected density of states (PDOS) of $Zn_{1-x}Co_xO$ ($x = 2.78$ %) when one hydrogen atom is doped. Unlike the hybridization by Co-3*d* and O-2*p* in Fig. 5, the spin polarization states of DOS at Fermi level originate from the coupling of H-1*s* and Co-3*d* bands. It is observed that the presence of hydrogen can increase the carriers concentration of system, which is similar to the results obtained by Roberts et al. [46]. Hydrogen atom tends to transfer electrons to the minority spin state of Co-3*d*, leading to a decrease of magnetic moment on Co ion.

To study the magnetic coupling, two Co atoms substituting for Zn are considered in 3×3×2 ZnO, corresponding

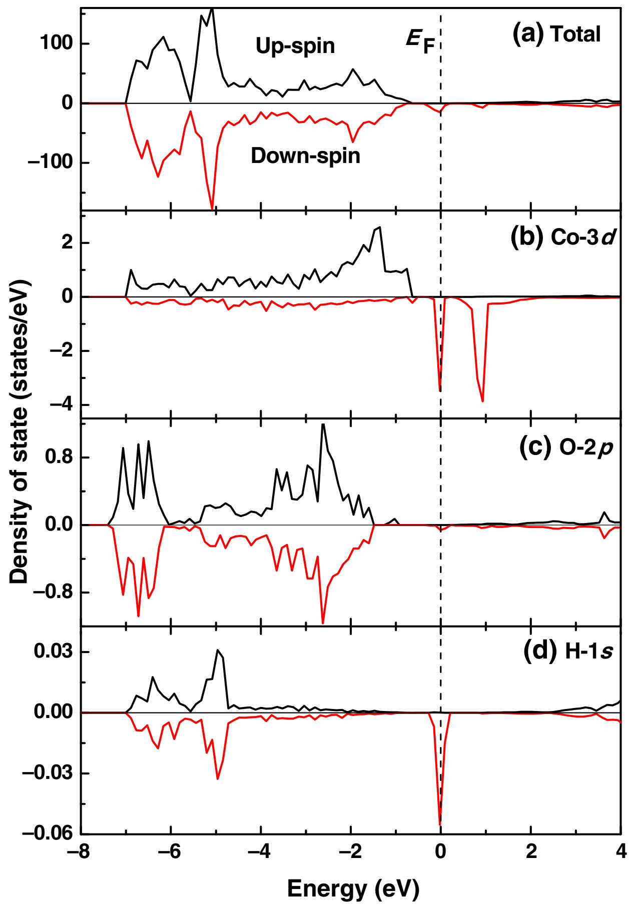

Fig. 6 (Color online) **a** Total density of states (DOS) and **b** Co-3*d* and **c** O-2*p* and **d** H-1*s* projected density of states (PDOS) of $Zn_{1-x}Co_xO$ ($x = 2.78$ %) (3×3×2 supercell) with hydrogen doped. The Fermi level (*dashed line*) is set as the zero energy. Positive (negative) values correspond to the majority (minority) spin

to a doped concentration of 5.55 %. We explore seven different configurations for Co atoms substitute at Zn sites marked (0, 1), (0, 2), (0, 3), (0, 4), (0, 5), (0, 6) and (0, 7), as seen in Fig. 2, respectively. Hydrogen atom is then present at interstitial $BC_{\perp}$ site near to the Co atom labeled 0. For each configuration, the total energies of the ferromagnetic (E_{FM}) and antiferromagnetic (E_{AFM}) spin configurations are calculated. The magnetic coupling strength *J* for the pair of Co atoms is then obtained from the energy difference between the FM and AFM configurations ($J = E_{AFM} - E_{FM}$). The magnetic coupling strengths will be also used as input parameters for Monte Carlo simulation. Figure 7 shows the magnetic coupling strength of the $Zn_{1-x}Co_xO$ ($x = 5.55$ %) for different configurations before and after hydrogen is doped. From the figure, it is found that the system has an FM ground state for all the configurations, which is consistent with previous reports [43, 47]. When hydrogen is doped, although the magnetic moment of system slightly decrease from 6.06 μ_B to 5.59 μ_B, the values of magnetic coupling strength *J* are found to be noticeably increased. Moreover, as the concentration of H^+ is enhanced, the magnetic moment of system greatly declines. The change trend is shown in Fig. 8, where the nearest neighbor configuration (0, 1) and the next neighbor configuration (0, 2) are considered due to their stronger Co-Co interaction among seven configurations. Figure 9(a) and (b) show the calculated magnetization *M* and U_L by Monte Carlo simulation for $Zn_{1-x}Co_xO$ ($x = 5.55$ %) without and with hydrogen doped, respectively. From the figures, it is observed that the Curie temperature T_c of $Zn_{1-x}Co_xO$ ($x = 5.55$ %) is about 200 K, near to experimental results [2, 48]. As hydrogen is

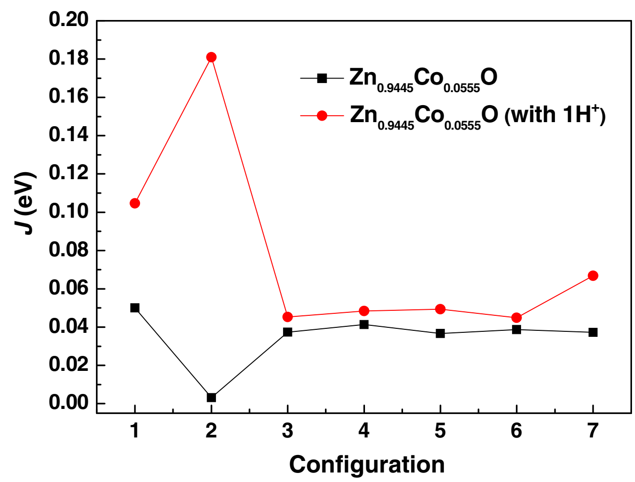

Fig. 7 (Color online) Magnetic coupling strength *J* between two substitutional Co of 7 configurations before and after hydrogen is doped

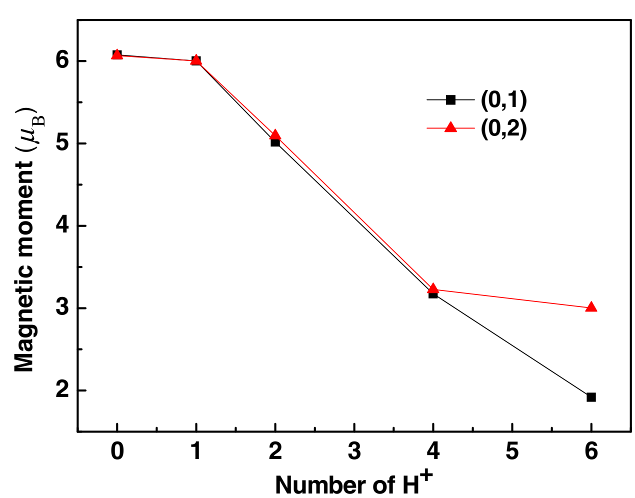

Fig. 8 (Color online) Magnetic moment as a function of number of doped H^+ for nearest neighbor configuration (0,1) and next nearest neighbor configuration (0,2) in the $Zn_{1-x}Co_xO$ ($x = 5.55$ %) system

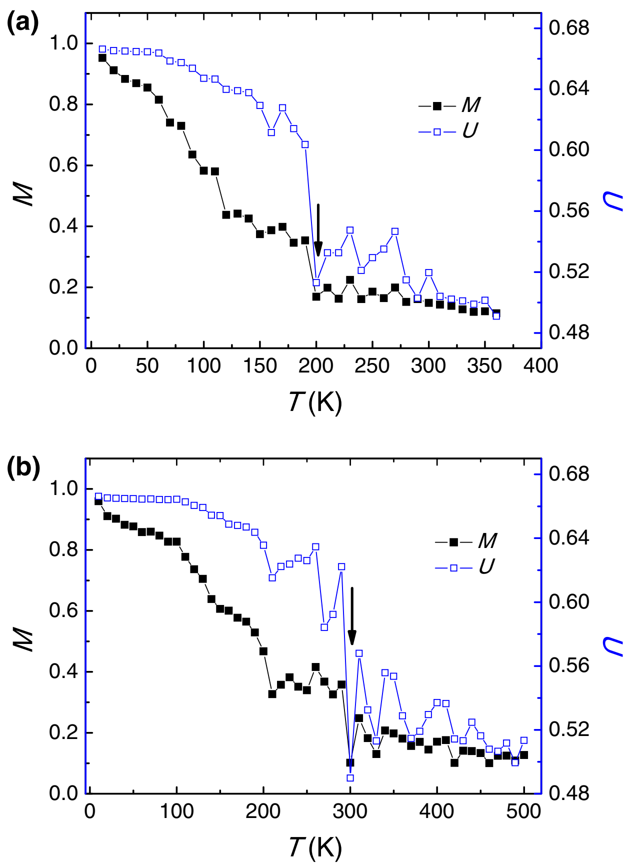

Fig. 9 (Color online) The simulated magnetization M and U_L as a function of temperature. **a** Without hydrogen doped, the T_c is 200 K. **b** With hydrogen doped, the T_c is 300 K

doped, a strong H-mediated spin-spin interaction can be induced [24], which leads to high temperature ferromagnetism with $T_c > 300$ K.

4 Conclusions

In this paper, the first-principle calculation and Monte Carlo simulation were employed to study the Co-doped ZnO diluted magnetic semiconductor with hydrogen doped. Bond-center (BC) sites were identified to be most stable sites for hydrogen, and the corresponding vibrational frequencies were calculated. The magnetic properties were investigated as well. The results reveal that hydrogen could lead to a change in electronic transfer, inducing the magnetic coupling changes, resulting in the increase of the Curie temperature from 200 to 300 K.

Acknowledgment The work was supported from the National Fundamental Research Program of China (2011CBA00200) and the National Natural Science Foundation of China (11074039 and 11204038).

References

1. Ohno H (1998) Making nonmagnetic semiconductors ferromagnetic. Science 281:951–956
2. Ueda K, Tabata H, Kawai T (2001) Magnetic and electric properties of transition-metal-doped ZnO films. Appl Phys Lett 79:988–990
3. Mofor AC, El-Shaer A, Bakin A et al (2005) Magnetic property investigations on Mn-doped ZnO layers on sapphire. Appl Phys Lett 87:062501
4. Xu HY, Liu YC, Xu CS et al (2006) Structural, optical, and magnetic properties of Mn-doped ZnO thin film. J Chem Phys 124:074707
5. Lee HJ, Jeong SY, Cho CS et al (2002) Study of diluted magnetic semiconductor: Co-doped ZnO. Appl Phys Lett 81:4020–4022
6. Weng ZZ, Zhang JM, Huang ZG et al (2011) Effect of oxygen vacancy defect on the magnetic properties of Co-doped ZnO. Chin Phys B 20:027103
7. Song C, Geng KW, Zeng F et al (2006) Giant magnetic moment in an anomalous ferromagnetic insulator: Co-doped ZnO. Phys Rev B 73:024405
8. Wang YQ, Yuan SL, Song YX et al (2007) Magnetism in Mn and Co doped ZnO bulk samples. Chin Sci Bull 52:1019–1023
9. Zhou SQ, Potzger K, Zhang GF et al (2006) Crystalline Ni nanoparticles as the origin of ferromagnetism in Ni implanted ZnO crystals. J Appl Phys 100:114304
10. Cong CJ, Hong JH, Liu QY et al (2006) Synthesis, structure and ferromagnetic properties of Ni-doped ZnO nanoparticles. Solid State Commun 138:511–515
11. Saeki H, Tabata H, Kawai T (2001) Magnetic and electric properties of vanadium doped ZnO films. Solid State Commun 120:439–443
12. Ramachandran S, Tiwari A, Narayan J et al (2005) Epitaxial growth and properties of $Zn_{1-x}V_xO$ diluted magnetic semiconductor thin films. Appl Phys Lett 87:172502
13. Hong NH, Sakai J, Hassini A (2005) Magnetic properties of V-doped ZnO thin films. J Appl Phys 97:10D312
14. Venkatesan M, Fitzgerald CB, Lunney JG et al (2004) Anisotropic ferromagnetism in substituted zinc oxide. Phys Rev Lett 93:177206
15. Hong NH, Sakai J, Huong NT et al (2005) Role of defects in tuning ferromagnetism in diluted magnetic oxide thin films. Phys Rev B 72:045336
16. Weng ZZ, Huang ZG, Lin WX (2012) Magnetism of Cr-doped ZnO with intrinsic defects. J Appl Phys 111:113915
17. Venkataraj S, Ohashi N, Sakaguchi I et al (2007) Structural and magnetic properties of Mn-ion implanted ZnO films. J Appl Phys 102:014905
18. Wei XX, Song C, Geng KW et al (2006) Local Fe structure and ferromagnetism in Fe-doped ZnO films. J Phys 18:7471–7479
19. Huang JCA, Hsu HS, Hu YM et al (2004) Origin of ferromagnetism in ZnO/CoFe multilayers: diluted magnetic semiconductor or clustering effect? Appl Phys Lett 85:3815–3817
20. Sati P, Hayn R, Kuzian R et al (2006) Magnetic anisotropy of Co^{2+} as signature of intrinsic ferromagnetism in ZnO:Co. Phys Rev Lett 96:017203
21. Neal JR, Behan AJ, Ibrahim RM et al (2006) Room-temperature magneto-optics of ferromagnetic transition-metal-doped ZnO thin films. Phys Rev Lett 96:197208
22. Risbud AS, Spaldin NA, Chen ZQ et al (2003) Magnetism in polycrystalline cobalt-substituted zinc oxide. Phys Rev B 68:205202
23. Lawes G, Risbud AS, Ramirez AP et al (2005) Absence of ferromagnetism in Co and Mn substituted polycrystalline ZnO. Phys Rev B 71:045201

24. Park CH, Chadi DJ (2005) Hydrogen-mediated spin-spin interaction in ZnCoO. Phys Rev Lett 94:127204
25. Deka S, Joy PA (2006) Ferromagnetism induced by hydrogen in polycrystalline nonmagnetic $Zn_{0.95}Co_{0.05}O$. Appl Phys Lett 89:032508
26. Lee HJ, Park CH, Jeong SY et al (2006) Hydrogen-induced ferromagnetism in ZnCoO. Appl Phys Lett 88:062504
27. Qiu H, Meyer B, Wang Y et al (2008) Ionization energies of shallow donor states in ZnO created by reversible formation and depletion of H interstitials. Phys Rev Lett 101:236401
28. Lavrov EV, Herklotz F, Weber J (2009) Identification of hydrogen molecules in ZnO. Phys Rev Lett 102:185502
29. Van de Walle CG (2000) Hydrogen as a cause of doping in zinc oxide. Phys Rev Lett 85:1012–1015
30. Hofmann DM, Hofstaetter A, Leiter F et al (2002) Hydrogen: a relevant shallow donor in zinc oxide. Phys Rev Lett 88:045504
31. Cox SFJ, Davis EA, Cottrell SP et al (2001) Experimental confirmation of the predicted shallow donor hydrogen state in zinc oxide. Phys Rev Lett 86:2601–2604
32. Khalid M, Esquinazi P (2012) Hydrogen-induced ferromagnetism in ZnO single crystals investigated by magnetotransport. Phys Rev B 85:134424
33. Li L, Guo Y, Cui XY et al (2012) Magnetism of Co-doped ZnO epitaxially grown on a ZnO substrate. Phys Rev B 85:174430
34. Kohn W, Sham LJ (1965) Self-consistent equations including exchange and correlation effects. Phys Rev 140:A1133–A1138
35. Blöchl PE (1994) Projector augmented-wave method. Phys Rev B 50:17953–17979
36. Kresse G, Hafner J (1993) *Ab initio* molecular dynamics for open-shell transition metals. Phys Rev B 48:13115–13118
37. Kresse G, Furthmuller (1996) Efficiency of ab-initio total energy calculations for metals and semiconductors using a plane-wave basis set. Compu Mater Sci 6:15–50
38. Van de Walle CG, Neugebauer J (2003) Universal alignment of hydrogen levels in semiconductors, insulators and solutions. Nature 423:626–628
39. Myers SM, Wright AF, Petersen GA et al (2000) Equilibrium state of hydrogen in gallium nitride: theory and experiment. J Appl Phys 88:4676–4687
40. Limpijumnong S, Northrup JE, Van de Walle CG (2003) Identification of hydrogen configurations in p-type GaN through first-principles calculations of vibrational frequencies. Phys Rev B 68:075206
41. Landau LD, Lifshitz EM (1977) Quantum mechanics. 3rd. Oxford: Pergamon, pp 136
42. Huang ZG, Chen ZG, Peng K et al (2004) Monte Carlo simulation of tunneling magnetoresistance in nanostructured materials. Phys Rev B 69:094420
43. Wu QY, Chen ZG, Wu R et al (2007) First-principles and monte carlo combinational study on $Zn_{1-x}Co_xO$ diluted magnetic semiconductor. Solid State Commun 142:242–246
44. Fukushima T, Sato K, Katayama-Yoshida H et al (2004) Theoretical prediction of curie temperature in (Zn, Cr)S, (Zn, Cr)Se and (Zn, Cr)Te by first principles calculations. Jpn J Appl Phys 43:L1416–L1418
45. Schliemann J, König J, MacDonald AH (2001) Monte carlo study of ferromagnetism in (III, Mn)V semiconductors. Phys Rev B 64:165201
46. Roberts BK, Pakhomov AB, Krishnan KM (2008) Effect of hydrogen codoping on magnetic ordering and conductivity in Cr:ZnO thin films. J Appl Phys 103:07D133
47. Sluiter MHF, Kawazoe Y, Sharma P et al (2005) First principles based design and experimental evidence for a ZnO-based ferromagnet at room temperature. Phys Rev Lett 94:187204
48. Fouchet A, Prellier W, Padhan P et al (2004) Structural and magnetic properties of a series of low-doped $Zn_{1-x}Co_xO$ thin films deposited from Zn and Co metal targets on (0001) Al_2O_3 substrates. J Appl Phys 95:7187–7189